Progress In Electromagnetics Research M, Vol. 49, 103–115, 2016

Propagation Properties of Partially Coherent Lorentz-Gauss Beams in Uniaxial Crystals Orthogonal to the X-Axis

Guoquan Zhou[1, *], Zhiyue Ji[1], and Guoyun Ru[2]

Abstract—Analytical expressions of the elements of a cross spectral density matrix are derived to describe the partially coherent Lorentz-Gauss beam propagating in uniaxial crystals orthogonal to the x-axis. The intensity and degree of polarization for the partially coherent Lorentz-Gauss beam propagating in uniaxial crystals orthogonal to the x-axis are also presented. The evolution properties of the partially coherent Lorentz-Gauss beam are numerically demonstrated. The influences of the uniaxial crystal and coherence length on the propagation properties of the partially coherent Lorentz-Gauss beam in uniaxial crystals orthogonal to the x-axis are examined. The uniaxial crystal considered here has the property of the extraordinary refractive index being larger than the ordinary refractive index. The partially coherent Lorentz-Gauss beam in the direction along the x-axis spreads more rapidly than that in the direction along the y-axis. With increasing the ratio of the extraordinary refractive index to the ordinary refractive index, the spreading of the partially coherent Lorentz-Gauss beam increases in the direction along the x-axis, but decreases in the direction along the y-axis. Meanwhile, the degree of polarization in the edges of the long and short axes of the beam spot increases. With increasing the coherence length, the beam spot of the partially coherent Lorentz-Gauss beam uniformly becomes less, and the maximum degree of polarization in the edge of the beam spot decreases.

1. INTRODUCTION

Due to high angular spreading, Lorentz-Gauss beams are introduced to describe the radiation emitted by a single mode laser diode [1, 2]. The beam properties including symmetry properties [3], focal shift [4], beam propagation factor [5], and Wigner distribution function [6, 7] of Lorentz-Gauss beams have been investigated, respectively. Also, the propagation of Lorentz-Gauss beams has been widely examined in free space [3], in uniaxial crystals orthogonal to the optical axis [8, 9], through a fractional Fourier transform optical system [10, 11], in a turbulent atmosphere [12], in a Kerr medium [13], and in a strongly nonlocal nonlinear media [14]. Tight focusing properties of radially polarized Lorentz-Gauss beam has been demonstrated [15]. A virtual source to generate the rotationally symmetric Lorentz-Gauss beam has been proposed [16]. The research also shows that the Lorentz-Gauss beam can be used to trap the particles with a refractive index larger than the ambient index [17].

In practical optical systems, laser beams are almost partially coherent [18], which indicates that fully coherent laser sources are ideal cases. Therefore, the research on Lorentz-Gauss beams has been further extended to partially coherent cases. Propagation of partially coherent Lorentz-Gauss beams through a paraxial $ABCD$ optical system has been investigated in free space and in a turbulent atmosphere, respectively [19, 20]. The scintillation aspects of partially coherent Lorentz-Gauss beams have been demonstrated via numerically integrating the average intensity and average squared intensity expressions [21]. The analytical expressions of the beam propagation factor and

Received 23 May 2016, Accepted 31 July 2016, Scheduled 8 August 2016

* Corresponding author: Guoquan Zhou (zhouguoquan178@sohu.com).

[1] School of Sciences, Zhejiang A & F University, Lin'an 311300, P. R. China. [2] ASML Inc., 77 Danbury Road, Wilton, CT 06897, USA.

the kurtosis parameter of a partially coherent Lorentz-Gauss beam have been derived in a turbulent atmosphere, respectively [22, 23]. An approximate analytical expression of the beam propagation factor for a truncated partially coherent Lorentz-Gauss beam has also been presented in free space [24].

Besides in free space, in a turbulent atmosphere and a nonlinear medium, laser beams also propagate in an anisotropic medium such as uniaxial crystal, which is treated by solving Maxwell's equations. Laser beams propagating in uniaxial crystals can be used not only to determine the crystal orientation, crystal structure, and mineral identification, but also to investigate crystal optical phenomena such as nonlinear effect and light scattering. Moreover, the design of the crystal optical element such as polarizing prism, optical compensator, and amplitude modulation device is also involved in laser beams propagating in uniaxial crystals. Although the propagation of various kinds of laser beams in uniaxial crystals has been reported [25–34], to the best of our knowledge, no literature has been reported on the propagation of partially coherent Lorentz-Gauss beams in uniaxial crystals. In the remainder of this paper, therefore, the propagation of the partially coherent Lorentz-Gauss beams in uniaxial crystals orthogonal to the x-axis is to be examined.

2. PROPAGATION OF THE PARTIALLY COHERENT LORENTZ-GAUSS BEAMS IN UNIAXIAL CRYSTALS ORTHOGONAL TO THE X-AXIS

In the Cartesian coordinate system, the z-axis is taken to be the propagation axis. The optical axis of the uniaxial crystal coincides with the x-axis. The boundary plane is $z = 0$. The ordinary and extraordinary refractive indices of the uniaxial crystal are n_o and n_e, respectively. The relative dielectric tensor of the uniaxial crystal reads as

$$\varepsilon = \begin{pmatrix} n_e^2 & 0 & 0 \\ 0 & n_o^2 & 0 \\ 0 & 0 & n_o^2 \end{pmatrix}, \tag{1}$$

The second order coherence and polarization properties of a partially coherent Lorentz-Gauss beam in the boundary plane $z = 0$ is characterized by the following 2×2 cross spectral density matrix [35]

$$\overleftrightarrow{W}(\boldsymbol{\rho}_{10}, \boldsymbol{\rho}_{20}, 0) = \begin{bmatrix} W_{xx}(\boldsymbol{\rho}_{10}, \boldsymbol{\rho}_{20}, 0) & W_{xy}(\boldsymbol{\rho}_{10}, \boldsymbol{\rho}_{20}, 0) \\ W_{yx}(\boldsymbol{\rho}_{10}, \boldsymbol{\rho}_{20}, 0) & W_{yy}(\boldsymbol{\rho}_{10}, \boldsymbol{\rho}_{20}, 0) \end{bmatrix}, \tag{2}$$

with the matrix element being given by

$$\begin{aligned} W_{ij}(\boldsymbol{\rho}_{10}, \boldsymbol{\rho}_{20}, 0) = {} & \frac{A_{ij} w_{0x}^2 w_{0y}^2}{\left(w_{0x}^2 + x_{10}^2\right)\left(w_{0y}^2 + y_{10}^2\right)\left(w_{0x}^2 + x_{20}^2\right)\left(w_{0y}^2 + y_{20}^2\right)} \exp\left(-\frac{x_{10}^2 + x_{20}^2 + y_{10}^2 + y_{20}^2}{w_0^2}\right) \\ & \times \exp\left[-\frac{(x_{10} - x_{20})^2 + (y_{10} - y_{20})^2}{\sigma^2}\right], \end{aligned} \tag{3}$$

where $\boldsymbol{\rho}_{10} = (x_{10}, y_{10})$ and $\boldsymbol{\rho}_{20} = (x_{20}, y_{20})$. w_{0x} and w_{0y} are the parameters related to the beam widths of the Lorentz part in the x- and y-directions, respectively. w_0 is the waist of the Gaussian part. σ is the coherence length. A_{ij} denotes the correlations of the x- and y-components. If $i = j$, $A_{ij} = 1$. If $i \neq j$, $|A_{ij}| \leq 1$. Moreover, $A_{ij}^* = A_{ji}$. The asterisk means the complex conjugation. The Lorentz distribution can be expanded into the linear superposition of Hermite-Gaussian functions [36]:

$$\begin{aligned} \frac{1}{\left(w_{0x}^2 + x_{10}^2\right)\left(w_{0y}^2 + y_{10}^2\right)} = {} & \frac{\pi}{2 w_{0x}^2 w_{0y}^2} \sum_{m_1=0}^{N} \sum_{n_1=0}^{N} a_{2m_1} a_{2n_1} H_{2m_1}\left(\frac{x_{10}}{w_{0x}}\right) H_{2n_1}\left(\frac{y_{10}}{w_{0y}}\right) \\ & \times \exp\left(-\frac{x_{10}^2}{2w_{0x}^2} - \frac{y_{10}^2}{2w_{0y}^2}\right), \end{aligned} \tag{4}$$

where N is the term number of the expansion. H_{2m_1} and H_{2n_1} are the $2m_1$-th and $2n_1$-th order Hermite polynomials, respectively. The weight coefficients a_{2m_1} and a_{2n_1} have been given by [36]. The value of a_{2m_1} dramatically decreases with increasing the even number $2m_1$. $a_0 = 0.7399$, $a_2 = 0.9298 \times 10^{-2}$,

and $a_{10} = 0.3008 \times 10^{-6}$. The cross spectral density matrix of the partially coherent Lorentz-Gauss beam propagating in uniaxial crystals orthogonal to the x-axis is found to be

$$\overleftrightarrow{W}(\boldsymbol{\rho}_1, \boldsymbol{\rho}_2, z) = \begin{bmatrix} W_{xx}(\boldsymbol{\rho}_1, \boldsymbol{\rho}_2, z) & W_{xy}(\boldsymbol{\rho}_1, \boldsymbol{\rho}_2, z) \\ W_{yx}(\boldsymbol{\rho}_1, \boldsymbol{\rho}_2, z) & W_{yy}(\boldsymbol{\rho}_1, \boldsymbol{\rho}_2, z) \end{bmatrix}, \tag{5}$$

where $\boldsymbol{\rho}_1 = (x_1, y_1)$ and $\boldsymbol{\rho}_2 = (x_2, y_2)$. As the scalar case is a simple one, here we only consider the scalar case. Within the framework of the paraxial propagation, the elements of the cross spectral density matrix propagating in uniaxial crystals orthogonal to the x-axis are given by [37, 38]

$$\begin{aligned} W_{xx}(\boldsymbol{\rho}_1, \boldsymbol{\rho}_2, z) &= \frac{k^2 n_o^2}{4\pi^2 z^2} \int_{-\infty}^{\infty}\int_{-\infty}^{\infty}\int_{-\infty}^{\infty}\int_{-\infty}^{\infty} W_{xx}(\boldsymbol{\rho}_{10}, \boldsymbol{\rho}_{20}, 0) \\ &\quad \times \exp\left\{\frac{ik}{2zn_e}\left[n_o^2(x_1 - x_{10})^2 + n_e^2(y_1 - y_{10})^2\right]\right\} \\ &\quad \times \exp\left\{\frac{-ik}{2zn_e}\left[n_o^2(x_2 - x_{20})^2 + n_e^2(y_2 - y_{20})^2\right]\right\} dx_{10}dy_{10}dx_{20}dy_{20}, \end{aligned} \tag{6}$$

$$\begin{aligned} W_{yy}(\boldsymbol{\rho}_1, \boldsymbol{\rho}_2, z) &= \frac{k^2 n_o^2}{4\pi^2 z^2} \int_{-\infty}^{\infty}\int_{-\infty}^{\infty}\int_{-\infty}^{\infty}\int_{-\infty}^{\infty} W_{yy}(\boldsymbol{\rho}_{10}, \boldsymbol{\rho}_{20}, 0) \exp\left\{\frac{ikn_o}{2z}\left[(x_1 - x_{10})^2 + (y_1 - y_{10})^2\right]\right\} \\ &\quad \times \exp\left\{\frac{-ikn_o}{2z}\left[(x_2 - x_{20})^2 + (y_2 - y_{20})^2\right]\right\} dx_{10}dy_{10}dx_{20}dy_{20}, \end{aligned} \tag{7}$$

$$\begin{aligned} W_{xy}(\boldsymbol{\rho}_1, \boldsymbol{\rho}_2, z) &= \frac{k^2 n_o^2}{4\pi^2 z^2} \exp\left[ikz(n_e - n_o)\right] \int_{-\infty}^{\infty}\int_{-\infty}^{\infty}\int_{-\infty}^{\infty}\int_{-\infty}^{\infty} W_{xy}(\boldsymbol{\rho}_{10}, \boldsymbol{\rho}_{20}, 0) \\ &\quad \times \exp\left\{\frac{ik}{2zn_e}\left[n_o^2(x_1 - x_{10})^2 + n_e^2(y_1 - y_{10})^2\right]\right\} \\ &\quad \times \exp\left\{\frac{-ikn_o}{2z}\left[(x_2 - x_{20})^2 + (y_2 - y_{20})^2\right]\right\} dx_{10}dy_{10}dx_{20}dy_{20}, \end{aligned} \tag{8}$$

$$W_{yx}(\boldsymbol{\rho}_1, \boldsymbol{\rho}_2, z) = W_{xy}^*(\boldsymbol{\rho}_1, \boldsymbol{\rho}_2, z), \tag{9}$$

where $k = 2\pi/\lambda$ is the wave number in vacuum and λ the incident wavelength in vacuum. Using the following mathematical formulae [39]:

$$\int_{-\infty}^{\infty} H_{2m'}(x) \exp\left[-(x-y)^2/u\right] dx = \sqrt{\pi/u}(1-u)^{m'} H_{2m'}\left[(1-u)^{-1/2}y\right], \tag{10}$$

$$H_{2m}(x) = \sum_{l=0}^{m} \frac{(-1)^l (2m)!}{l!(2m-2l)!}(2x)^{2m-2l}, \tag{11}$$

$$(a+b)^n = \sum_{l=0}^{n} \frac{n!}{l!(n-l)!} a^{n-l} b^l, \tag{12}$$

$$\int_{-\infty}^{\infty} x^{2n} \exp\left(-bx^2 + 2cx\right) dx = (2n)! \sqrt{\frac{\pi}{b}} \left(\frac{c}{b}\right)^{2n} \exp\left(\frac{c^2}{b}\right) \sum_{s=0}^{n} \frac{1}{s!(2n-2s)!} \left(\frac{b}{4c^2}\right)^s, \tag{13}$$

the elements of the cross spectral density matrix propagating in uniaxial crystals orthogonal to the x-axis can be analytically expressed as

$$\begin{aligned} W_{xx}(\boldsymbol{\rho}_1, \boldsymbol{\rho}_2, z) &= \frac{k^2\pi^2 n_o^2}{16z^2} \sqrt{\frac{b_1 u_1}{b_2 u_2}} \exp\left[\frac{ik}{2zn_e}\left[n_o^2(x_1^2 - x_2^2) + n_e^2(y_1^2 - y_2^2)\right]\right] \exp\left[-\frac{1}{4b_1}\left(\frac{kn_o^2 w_{0x} x_1}{zn_e}\right)^2\right] \\ &\quad \times \exp\left[-\frac{1}{4u_1}\left(\frac{kn_e w_{0y} y_1}{z}\right)^2\right] \sum_{m_1=0}^{N}\sum_{n_1=0}^{N}\sum_{m_2=0}^{N}\sum_{n_2=0}^{N} a_{2m_1} a_{2n_1} a_{2m_2} a_{2n_2} \left(1 - \frac{1}{b_1}\right)^{m_1} \\ &\quad \times \sum_{l_1=0}^{m_1} \frac{(-1)^{l_1}(2m_1)!}{l_1!(2m_1-2l_1)!(b_1^2-b_1)^{m_1-l_1}} \sum_{l_2=0}^{2m_1-2l_1} \frac{(2m_1-2l_1)!}{l_2!(2m_1-2l_1-l_2)!} \left(\frac{ikn_o^2 w_{0x} x_1}{zn_e}\right)^{2m_1-2l_1-l_2} \end{aligned}$$

$$\times\left(-\frac{2w_{0x}^2}{\sigma^2}\right)^{l_2}\sum_{l_3=0}^{m_2}\frac{(-1)^{l_3}(2m_2)!}{l_3!(2m_2-2l_3)!}2^{2m_2-2l_3}(2m_2-2l_3+l_2)!\left(\frac{c_1}{b_2}\right)^{2m_2-2l_3+l_2}\exp\left(\frac{c_1^2}{b_2}\right)$$
$$\times\sum_{s_1=0}^{[(2m_2-2l_3+l_2)/2]}\frac{1}{s_1!(2m_2-2l_3+l_2-2s_1)!}\left(\frac{b_2}{4c_1^2}\right)^{s_1}\left(1-\frac{1}{u_1}\right)^{n_1}$$
$$\times\sum_{l_4=0}^{n_1}\frac{(-1)^{l_4}(2n_1)!}{l_4!(2n_1-2l_4)!(u_1^2-u_1)^{n_1-l_4}}\sum_{l_5=0}^{2n_1-2l_4}\frac{(2n_1-2l_4)!}{l_5!(2n_1-2l_4-l_5)!}$$
$$\times\left(\frac{ikn_ew_{0y}y_1}{z}\right)^{2n_1-2l_4-l_5}\left(-\frac{2w_{0y}^2}{\sigma^2}\right)^{l_5}\sum_{l_6=0}^{n_2}\frac{(-1)^{l_6}(2n_2)!}{l_6!(2n_2-2l_6)!}2^{2n_2-2l_6}(2n_2-2l_6+l_5)!$$
$$\times\left(\frac{c_2}{u_2}\right)^{2n_2-2l_6+l_5}\exp\left(\frac{c_2^2}{u_2}\right)\sum_{s_2=0}^{[(2n_2-2l_6+l_5)/2]}\frac{1}{s_2!(2n_2-2l_6+l_5-2s_2)!}\left(\frac{u_2}{4c_2^2}\right)^{s_2}, \quad (14)$$

$$W_{yy}(\boldsymbol{\rho}_1,\boldsymbol{\rho}_2,z) = \frac{k^2\pi^2n_o^2}{16z^2}\sqrt{\frac{b_3u_3}{b_4u_4}}\exp\left[\frac{ikn_o}{2z}(\rho_1^2-\rho_2^2)\right]\exp\left[-\frac{1}{4b_3}\left(\frac{kn_ow_{0x}x_1}{z}\right)^2-\frac{1}{4u_3}\left(\frac{kn_ow_{0y}y_1}{z}\right)^2\right]$$
$$\times\sum_{m_1=0}^{N}\sum_{n_1=0}^{N}\sum_{m_2=0}^{N}\sum_{n_2=0}^{N}a_{2m_1}a_{2n_1}a_{2m_2}a_{2n_2}\left(1-\frac{1}{b_3}\right)^{m_1}\sum_{l_1=0}^{m_1}\frac{(-1)^{l_1}(2m_1)!}{l_1!(2m_1-2l_1)!(b_3^2-b_3)^{m_1-l_1}}$$
$$\times\sum_{l_2=0}^{2m_1-2l_1}\frac{(2m_1-2l_1)!}{l_2!(2m_1-2l_1-l_2)!}\left(\frac{ikn_ow_{0x}x_1}{z}\right)^{2m_1-2l_1-l_2}\left(-\frac{2w_{0x}^2}{\sigma^2}\right)^{l_2}\sum_{l_3=0}^{m_2}\frac{(-1)^{l_3}(2m_2)!}{l_3!(2m_2-2l_3)!}$$
$$\times2^{2m_2-2l_3}(2m_2-2l_3+l_2)!\left(\frac{c_3}{b_4}\right)^{2m_2-2l_3+l_2}$$
$$\times\exp\left(\frac{c_3^2}{b_4}\right)\sum_{s_1=0}^{[(2m_2-2l_3+l_2)/2]}\frac{1}{s_1!(2m_2-2l_3+l_2-2s_1)!}$$
$$\times\left(\frac{b_4}{4c_3^2}\right)^{s_1}\left(1-\frac{1}{u_3}\right)^{n_1}\sum_{l_4=0}^{n_1}\frac{(-1)^{l_4}(2n_1)!}{l_4!(2n_1-2l_4)!(u_3^2-u_3)^{n_1-l_4}}\sum_{l_5=0}^{2n_1-2l_4}\frac{(2n_1-2l_4)!}{l_5!(2n_1-2l_4-l_5)!}$$
$$\times\left(\frac{ikn_ow_{0y}y_1}{z}\right)^{2n_1-2l_4-l_5}\left(-\frac{2w_{0y}^2}{\sigma^2}\right)^{l_5}\sum_{l_6=0}^{2n_2}\frac{(-1)^{l_6}(2n_2)!}{l_6!(2n_2-2l_6)!}2^{2n_2-2l_6}(2n_2-2l_6+l_5)!$$
$$\times\left(\frac{c_4}{u_4}\right)^{2n_2-2l_6+l_5}\exp\left(\frac{c_4^2}{u_4}\right)\sum_{s_2=0}^{[(2n_2-2l_6+l_5)/2]}\frac{1}{s_2!(2n_2-2l_6+l_5-2s_2)!}\left(\frac{u_4}{4c_4^2}\right)^{s_2}, \quad (15)$$

$$W_{xy}(\boldsymbol{\rho}_1,\boldsymbol{\rho}_2,z) = \frac{k^2\pi^2n_o^2A_{xy}}{16^2z^2}\sqrt{\frac{b_1u_1}{b_5u_5}}\exp[ikz(n_e-n_o)]\exp\left(\frac{ikn_o^2}{2zn_e}x_1^2+\frac{ikn_e}{2z}y_1^2-\frac{ikn_o}{2z}\rho_2^2\right)$$
$$\times\exp\left[-\frac{1}{4b_1}\left(\frac{kn_o^2w_{0x}x_1}{zn_e}\right)^2-\frac{1}{4u_1}\left(\frac{kn_ew_{0y}y_1}{z}\right)^2\right]$$
$$\times\sum_{m_1=0}^{N}\sum_{n_1=0}^{N}\sum_{m_2=0}^{N}\sum_{n_2=0}^{N}a_{2m_1}a_{2n_1}a_{2m_2}a_{2n_2}\left(1-\frac{1}{b_1}\right)^{m_1}\sum_{l_1=0}^{m_1}\frac{(-1)^{l_1}(2m_1)!}{l_1!(2m_1-2l_1)!(b_1^2-b_1)^{m_1-l_1}}$$
$$\times\sum_{l_2=0}^{2m_1-2l_1}\frac{2m_1-2l_1!}{l_2!(2m_1-2l_1-l_2)!}\left(\frac{ikn_o^2w_{0x}x_1}{zn_e}\right)^{2m_1-2l_1-l_2}$$

$$\left(-\frac{2w_{0x}^2}{\sigma^2}\right)^{l_2}\sum_{l_3=0}^{m_2}\frac{(-1)^{l_3}(2m_2)!}{l_3!(2m_2-2l_3)!}2^{2m_2-2l_3}$$
$$\times(2m_2-2l_3+l_2)!\left(\frac{c_5}{b_5}\right)^{2m_2-2l_3+l_2}\exp\left(\frac{c_5^2}{b_5}\right)\sum_{s_1=0}^{[(2m_2-2l_3+l_2)/2]}\frac{1}{s_1!(2m_2-2l_3+l_2-2s_1)!}\left(\frac{b_5}{4c_5^2}\right)^{s_1}$$
$$\times\left(1-\frac{1}{u_1}\right)^{n_1}\sum_{l_4=0}^{n_1}\frac{(-1)^{l_4}(2n_1)!}{l!(2n_1-2l_4)!(u_1^2-u_1)^{n_1-l_4}}\sum_{l_5=0}^{2n_1-2l_4}\frac{(2n_1-2l_4)!}{l_5!(2n_1-2l_4-l_5)!}\left(\frac{ikn_ew_{0y}y_1}{z}\right)^{2n_1-2l_4-l_5}$$
$$\times\left(-\frac{2w_{0y}^2}{\sigma^2}\right)^{l_5}\sum_{l_6=0}^{n_2}\frac{(-1)^{l_6}(2n_2)!}{l_6!(2n_2-2l_6)!}2^{2n_2-2l_6}(2n_2-2l_6+l_5)!\left(\frac{c_6}{u_5}\right)^{2n_2-2l_6+l_5}\exp\left(\frac{c_6^2}{u_5}\right)$$
$$\times\sum_{s_2=0}^{[(2n_2-2l_6+l_5)/2]}\frac{1}{s_2!(2n_2-2l_6+l_5-2s_2)!}\left(\frac{u_5}{4c_6^2}\right)^{s_2}, \tag{16}$$

where the auxiliary parameters are defined as follows:

$$b_1 = \left(\frac{1}{w_0^2}+\frac{1}{2w_{0x}^2}+\frac{1}{\sigma^2}-\frac{ikn_o^2}{2zn_e}\right)w_{0x}^2, \tag{17}$$
$$b_2 = \left(\frac{1}{w_0^2}+\frac{1}{2w_{0x}^2}+\frac{1}{\sigma^2}+\frac{ikn_o^2}{2zn_e}\right)w_{0x}^2-\frac{w_{0x}^4}{b_1\sigma^4}, \tag{18}$$
$$c_1 = \frac{ikw_{0x}n_o^2x_2}{2n_ez}-\frac{ikw_{0x}^3n_o^2x_1}{2b_1\sigma^2n_ez}, \tag{19}$$
$$u_1 = \left(\frac{1}{w_0^2}+\frac{1}{2w_{0y}^2}+\frac{1}{\sigma^2}-\frac{ikn_e}{2z}\right)w_{0y}^2, \tag{20}$$
$$u_2 = \left(\frac{1}{w_0^2}+\frac{1}{2w_{0y}^2}+\frac{1}{\sigma^2}+\frac{ikn_e}{2z}\right)w_{0y}^2-\frac{w_{0y}^4}{u_1\sigma^4}, \tag{21}$$
$$c_2 = \frac{ikw_{0y}n_ey_2}{2z}-\frac{ikw_{0y}^3n_ey_1}{2u_1\sigma^2z}, \tag{22}$$
$$b_3 = \left(\frac{1}{w_0^2}+\frac{1}{2w_{0x}^2}+\frac{1}{\sigma^2}-\frac{ikn_o}{2z}\right)w_{0x}^2, \tag{23}$$
$$b_4 = \left(\frac{1}{w_0^2}+\frac{1}{2w_{0x}^2}+\frac{1}{\sigma^2}+\frac{ikn_o}{2z}\right)w_{0x}^2-\frac{w_{0x}^4}{b_3\sigma^4}, \tag{24}$$
$$c_3 = \frac{ikw_{0x}n_ox_2}{2z}-\frac{ikw_{0x}^3n_ox_1}{2b_3\sigma^2z}, \tag{25}$$
$$u_3 = \left(\frac{1}{w_0^2}+\frac{1}{2w_{0y}^2}+\frac{1}{\sigma^2}-\frac{ikn_o}{2z}\right)w_{0y}^2, \tag{26}$$
$$u_4 = \left(\frac{1}{w_0^2}+\frac{1}{2w_{0y}^2}+\frac{1}{\sigma^2}+\frac{ikn_o}{2z}\right)w_{0y}^2-\frac{w_{0y}^4}{u_3\sigma^4}, \tag{27}$$
$$c_4 = \frac{ikw_{0y}n_oy_2}{2z}-\frac{ikw_{0y}^3n_oy_1}{2u_3\sigma^2z}, \tag{28}$$
$$c_5 = \frac{ikw_{0x}n_ox_2}{2z}-\frac{ikw_{0x}^3n_o^2x_1}{2b_1\sigma^2n_ez}, \tag{29}$$

$$b_5 = \left(\frac{1}{w_0^2} + \frac{1}{2w_{0x}^2} + \frac{1}{\sigma^2} + \frac{ikn_o}{2z}\right) w_{0x}^2 - \frac{w_{0x}^4}{b_1\sigma^4}, \tag{30}$$

$$u_5 = \left(\frac{1}{w_0^2} + \frac{1}{2w_{0y}^2} + \frac{1}{\sigma^2} + \frac{ikn_o}{2z}\right) w_{0y}^2 - \frac{w_{0y}^4}{u_1\sigma^4}, \tag{31}$$

$$c_6 = \frac{ikw_{0y}n_o y_2}{2z} - \frac{ikw_{0y}^3 n_e y_1}{2u_1\sigma^2 z}. \tag{32}$$

The intensity and degree of polarization for the partially coherent Lorentz-Gauss beam propagating in uniaxial crystals orthogonal to the x-axis are given by [35]

$$I(\boldsymbol{\rho}, z) = \mathrm{Tr}\overleftrightarrow{W}(\boldsymbol{\rho}, \boldsymbol{\rho}, z) = W_{xx}(\boldsymbol{\rho}, \boldsymbol{\rho}, z) + W_{yy}(\boldsymbol{\rho}, \boldsymbol{\rho}, z), \tag{33}$$

$$P(\boldsymbol{\rho}, z) = \left\{1 - \frac{4\mathrm{det}\overleftrightarrow{W}(\boldsymbol{\rho}, \boldsymbol{\rho}, z)}{[\mathrm{Tr}\overleftrightarrow{W}(\boldsymbol{\rho}, \boldsymbol{\rho}, z)]^2}\right\}^{1/2}, \tag{34}$$

where Tr denotes the trace, and det stands for the determinant.

3. NUMERICAL CALCULATIONS AND ANALYSES

According to the obtained analytical expressions (Equations (14)–(16)), the properties of the partially coherent Lorentz-Gauss beam propagating in uniaxial crystals orthogonal to the x-axis are numerically demonstrated. The calculation parameters are set as follows: $\lambda = 0.8\,\mu\mathrm{m}$, $w_0 = 20\,\mu\mathrm{m}$, $w_{0x} = w_{0y} = 10\,\mu\mathrm{m}$, and $n_o = 2.616$ (rutile crystal). Fig. 1 represents the normalized intensity distribution of the partially coherent Lorentz-Gauss beam in different observation planes of the uniaxial crystal. $z_0 = kw_0^2/2$ is the Rayleigh distance in vacuum. $\sigma = 10\,\mu\mathrm{m}$ and $n_e/n_o = 1.1$ in Fig. 1. Equation (33) denotes that the intensity of the partially coherent Lorentz-Gauss beam is independent of A_{xy}. Upon propagation

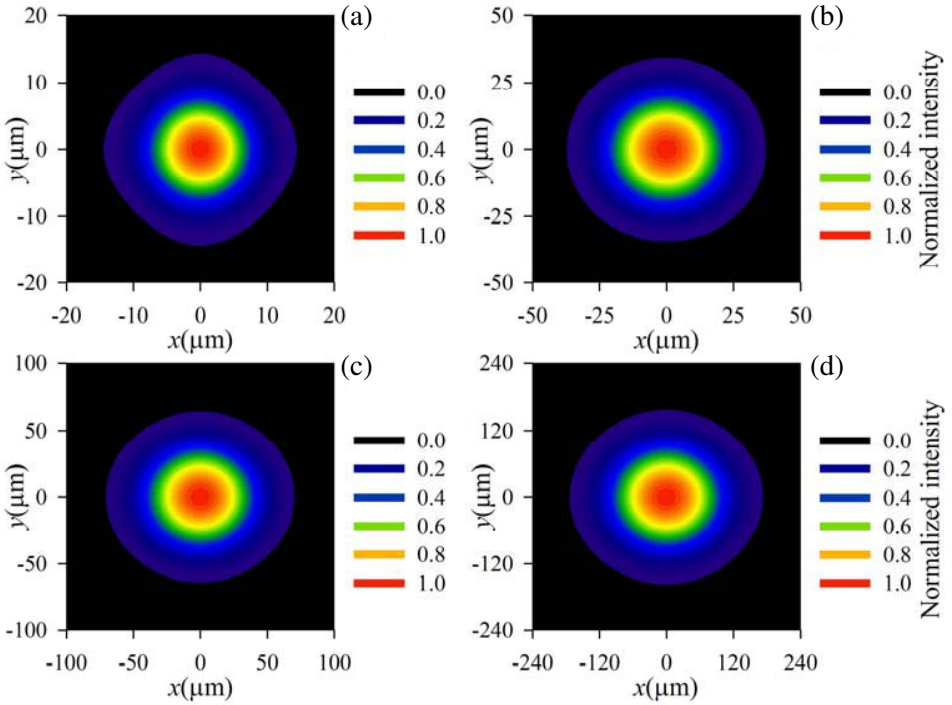

Figure 1. The normalized intensity distribution of the partially coherent Lorentz-Gauss beam propagating in the uniaxial crystal. $\sigma = 10\,\mu\mathrm{m}$ and $n_e/n_o = 1.1$. (a) $z = 0.1z_0$, (b) $z = z_0$, (c) $z = 2z_0$, and (d) $z = 5z_0$.

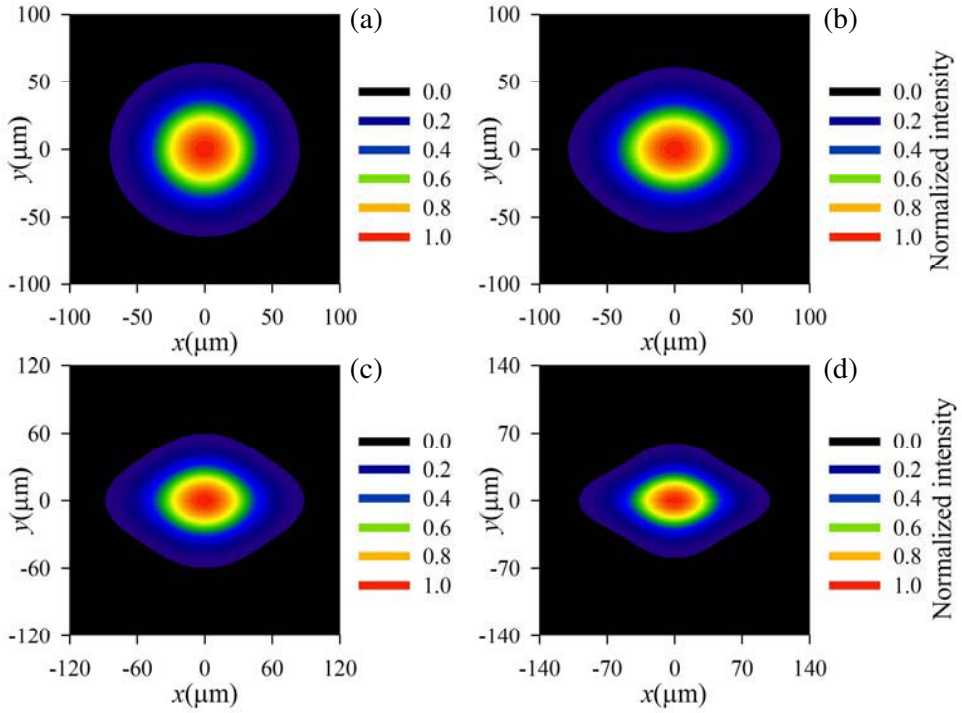

Figure 2. The normalized intensity distribution of the partially coherent Lorentz-Gauss beam propagating in different uniaxial crystal. $\sigma = 10\,\mu\text{m}$ and $z = 2z_0$. (a) $n_e/n_o = 1.1$, (b) $n_e/n_o = 1.3$, (c) $n_e/n_o = 1.5$, and (d) $n_e/n_o = 1.7$.

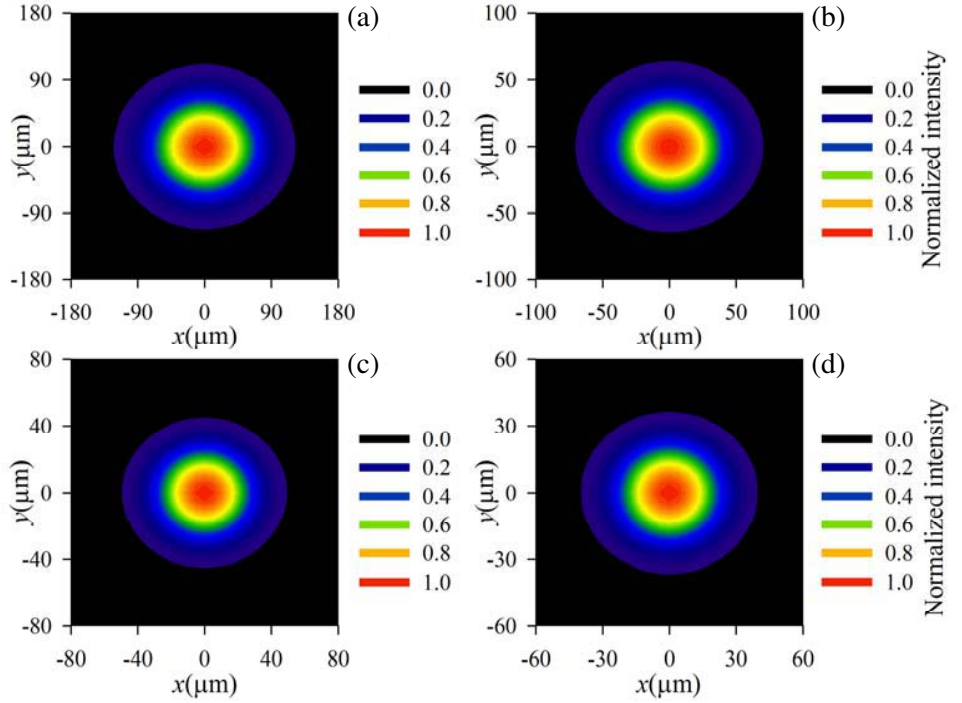

Figure 3. The normalized intensity distribution of the partially coherent Lorentz-Gauss beam propagating in the uniaxial crystal. $n_e/n_o = 1.1$ and $z = 2z_0$. (a) $\sigma = 5\,\mu\text{m}$, (b) $\sigma = 10\,\mu\text{m}$, (c) $\sigma = 20\,\mu\text{m}$, and (d) $\sigma = \infty$.

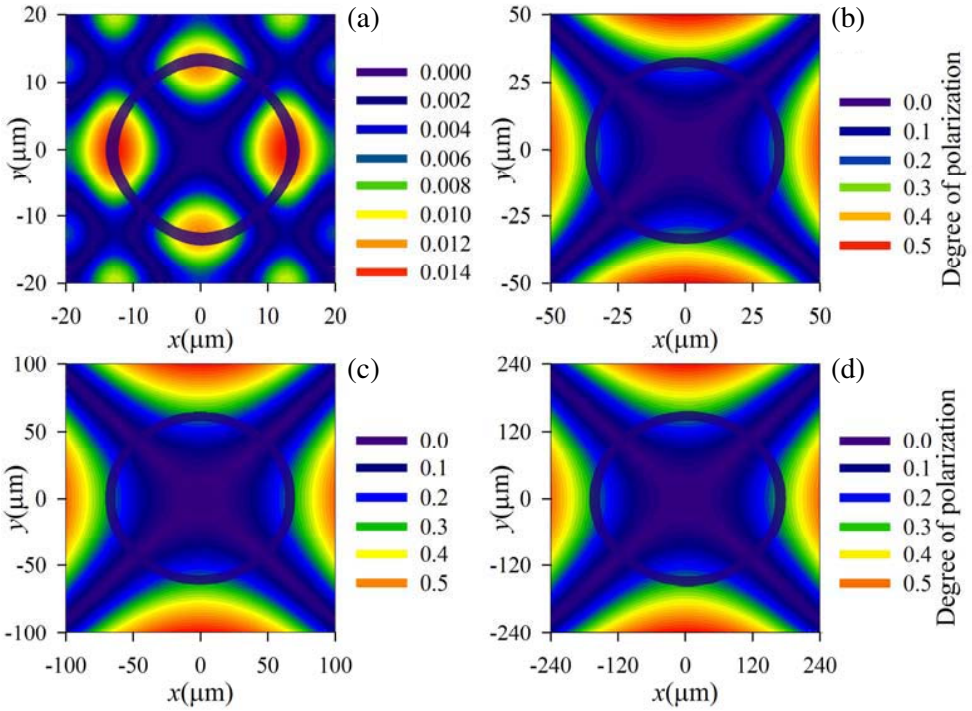

Figure 4. The distribution of the degree of polarization of the partially coherent Lorentz-Gauss beam propagating in the uniaxial crystal. $A_{xy} = 0$, $\sigma = 10\,\mu\text{m}$, and $n_e/n_o = 1.1$. (a) $z = 0.1z_0$, (b) $z = z_0$, (c) $z = 2z_0$, and (d) $z = 5z_0$.

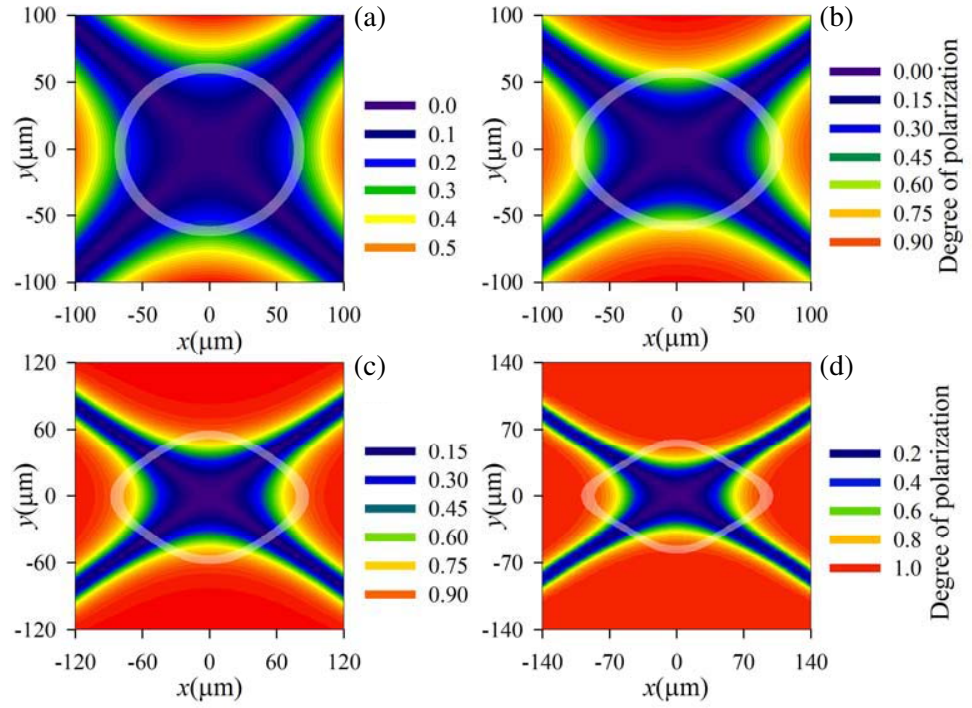

Figure 5. The distribution of the degree of polarization of the partially coherent Lorentz-Gauss beam propagating in different uniaxial crystal. $A_{xy} = 0$, $\sigma = 10\,\mu\text{m}$, and $z = 2z_0$. (a) $n_e/n_o = 1.1$, (b) $n_e/n_o = 1.3$, (c) $n_e/n_o = 1.5$, and (d) $n_e/n_o = 1.7$.

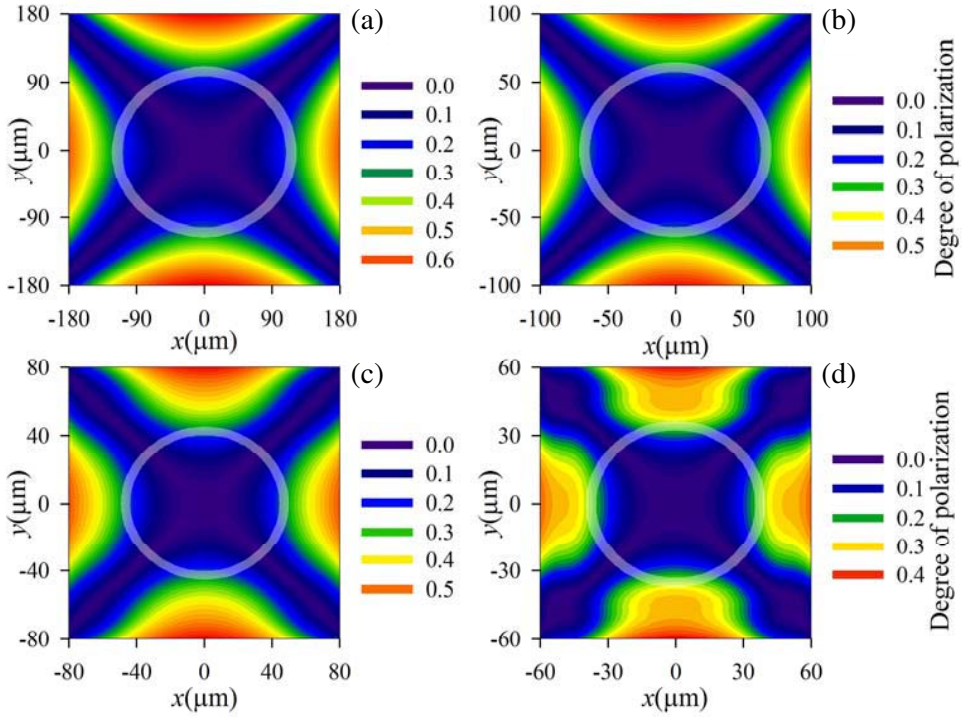

Figure 6. The distribution of the degree of polarization of the partially coherent Lorentz-Gauss beam propagating in the uniaxial crystal. $A_{xy} = 0$, $n_e/n_o = 1.1$, and $z = 2z_0$. (a) $\sigma = 5\,\mu\text{m}$, (b) $\sigma = 10\,\mu\text{m}$, (c) $\sigma = 20\,\mu\text{m}$, and (d) $\sigma = \infty$.

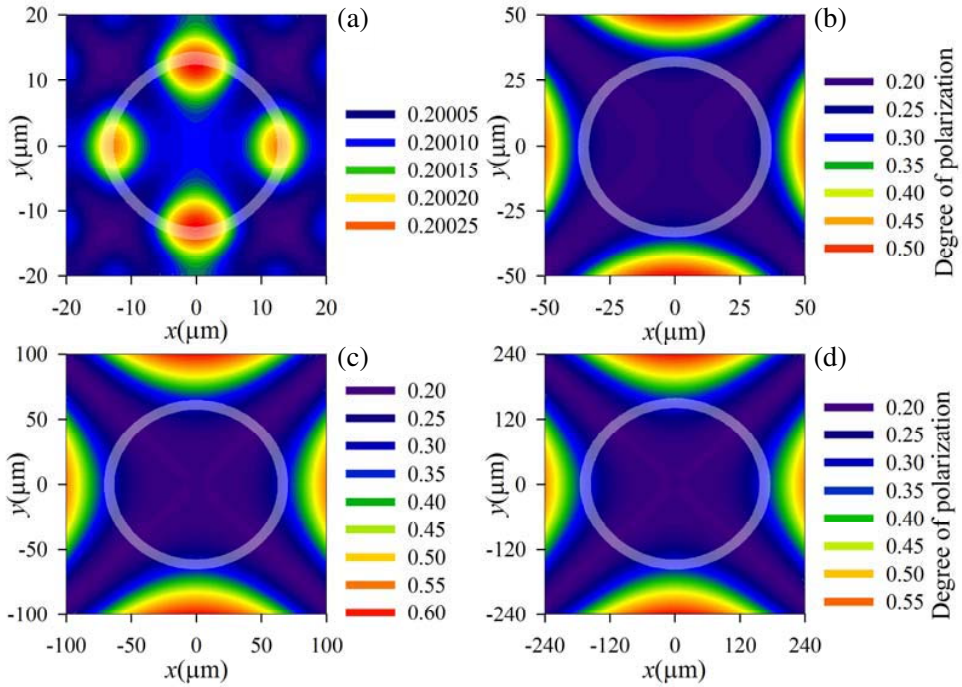

Figure 7. The distribution of the degree of polarization of the partially coherent Lorentz-Gauss beam propagating in the uniaxial crystal. $A_{xy} = 0.2$, $\sigma = 10\,\mu\text{m}$, and $n_e/n_o = 1.1$. (a) $z = 0.1z_0$, (b) $z = z_0$, (c) $z = 2z_0$, and (d) $z = 5z_0$.

in the uniaxial crystals orthogonal to the x-axis, the spreading of the partially coherent Lorentz-Gauss beam in the direction along the y-axis is far slower than that in the direction along the x-axis due to anisotropic effect of the crystals. As a result, the beam spot of the partially coherent Lorentz-Gauss beam propagating in the uniaxial crystals is elongated in the direction along the x-axis. The normalized intensity distribution of the partially coherent Lorentz-Gauss beam propagating in different uniaxial crystals is shown in Fig. 2. $\sigma = 10\,\mu\text{m}$ and $z = 2z_0$ in Fig. 2. With increasing the value of n_e/n_o, the spreading of the partially coherent Lorentz-Gauss beam increases in the direction along the x-axis, but decreases in the direction along y-axis, which results in the increased elongation of the beam spot in the direction along the x-axis. Fig. 3 represents the normalized intensity distribution of the partially coherent Lorentz-Gauss beam with different coherence lengths in the observation plane $z = 2z_0$. $n_e/n_o = 1.1$ in Fig. 3. With increasing the coherence length, the beam spot of the partially coherent Lorentz-Gauss beam shrinks uniformly in each direction. Therefore, the beam spot of a fully coherent Lorentz-Gauss beam is the smallest.

Figure 4 represents the distribution of degree of polarization of the partially coherent Lorentz-Gauss beam in different observation planes of the uniaxial crystal. $A_{xy} = 0$, $\sigma = 10\,\mu\text{m}$, and $n_e/n_o = 1.1$ in Fig. 4. The loop in the subfigures denotes that the normalized intensity inside it is not equal to zero (hereafter). Here, we only discuss the degree of polarization at the region where the normalized intensity distribution is larger than zero. The degree of polarization shows a symmetrical distribution. The degree of polarization in the edges of the long and short axes reaches the maximum and second largest values, respectively. As $A_{xy} = 0$, the on-axis degree of polarization is always zero. Moreover, the degree of polarization in the central region of the beam spot is also equal to zero. Upon propagation in the uniaxial crystals orthogonal to the x-axis, the degree of polarization in the edge of the beam spot first increases and then keeps stable without considering the expansion of the beam spot.

The degree of polarization of the partially coherent Lorentz-Gauss beam propagating in different uniaxial crystals has different distribution, as shown in Fig. 5, in which $A_{xy} = 0$, $\sigma = 10\,\mu\text{m}$, and $z = 2z_0$. It is shown that the degree of polarization in the edges of the long and short axes increases with the increase of n_e/n_o. With increasing the value of n_e/n_o, the region along the x-axis where the degree of polarization has the maximum value increases faster than the region along the y-axis where

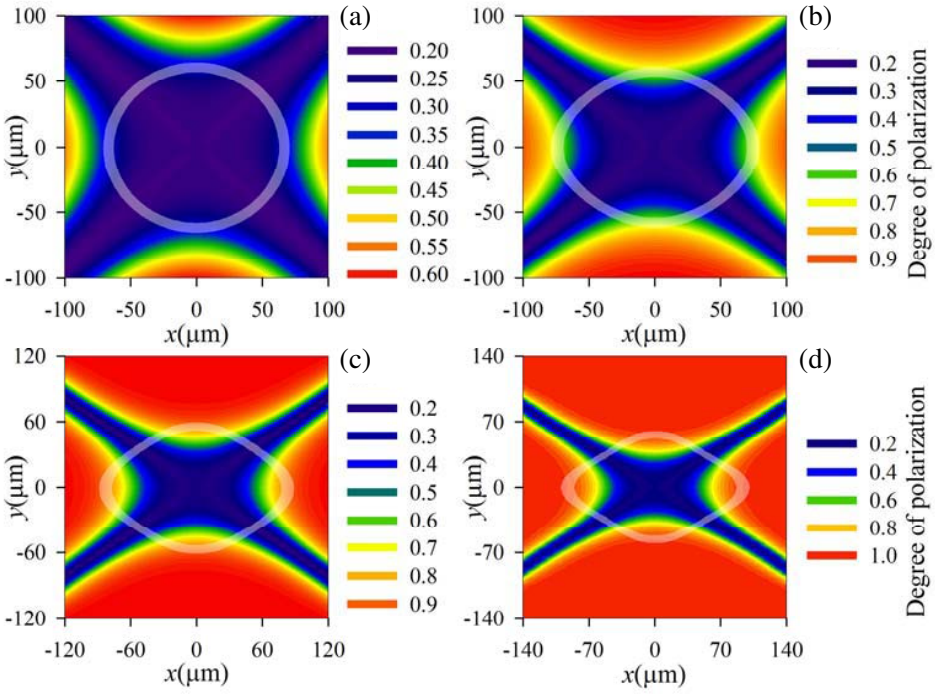

Figure 8. The distribution of the degree of polarization of the partially coherent Lorentz-Gauss beam propagating in different uniaxial crystal. $A_{xy} = 0.2$, $\sigma = 10\,\mu\text{m}$, and $z = 2z_0$. (a) $n_e/n_o = 1.1$, (b) $n_e/n_o = 1.3$, (c) $n_e/n_o = 1.5$, and (d) $n_e/n_o = 1.7$.

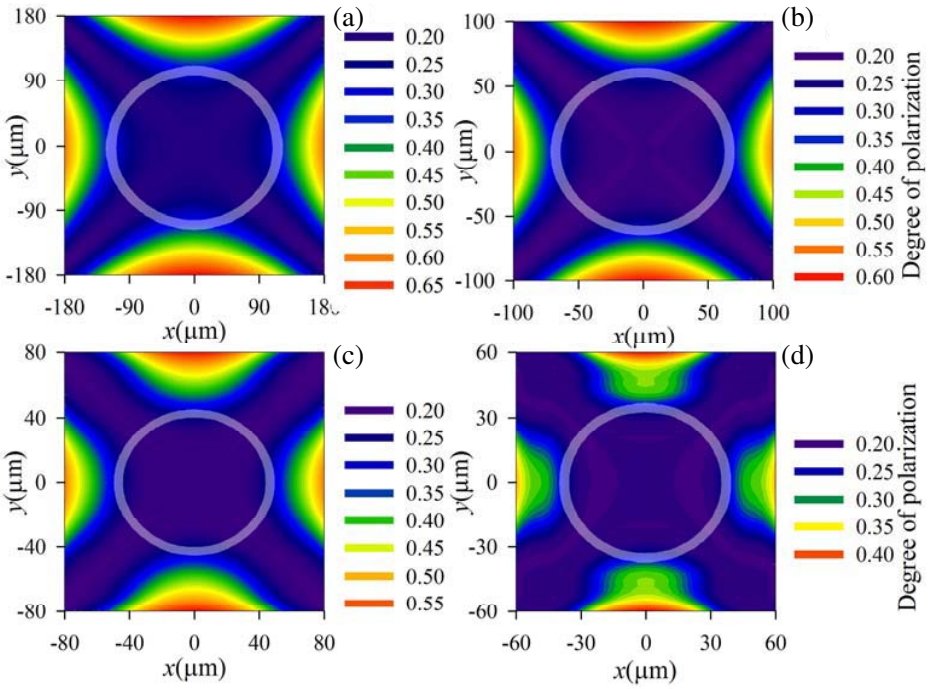

Figure 9. The distribution of the degree of polarization of the partially coherent Lorentz-Gauss beam propagating in the uniaxial crystal. $A_{xy} = 0.2$, $n_e/n_o = 1.1$, and $z = 2z_0$. (a) $\sigma = 5\,\mu$m, (b) $\sigma = 10\,\mu$m, (c) $\sigma = 20\,\mu$m, and (d) $\sigma = \infty$.

the degree of polarization has the maximum value. With increasing the value of n_e/n_o, therefore, the region difference where the degree of polarization has the maximum value between the directions along the x- and y-axes widens. The region with the maximal value of the degree of polarization in the direction along the x-axis is larger than that in the direction along the y-axis. Fig. 6 represents the distribution of the degree of polarization of the partially coherent Lorentz-Gauss beam with different coherence lengths in the observation plane $z = 2z_0$. $A_{xy} = 0$ and $n_e/n_o = 1.1$ in Fig. 6. The magnitude of the degree of polarization in Fig. 6(c) is larger than that in Fig. 6(b). However, their difference is slightly smaller than 0.1, which leads to their same label in Fig. 6. With increasing the coherence length, the maximum degree of polarization in the edge of the beam spot will decrease. As a result, the degree of polarization of the fully coherent Lorentz-Gauss beam reaches the smallest value. Figs. 7–9 are very similar to Figs. 4–6, respectively. The only difference is that $A_{xy} = 0$ in Figs. 4–6 and $A_{xy} = 0.2$ in Figs. 7–9. Comparing Figs. 7–9 with Figs. 4–6, one can draw a conclusion that all the results obtained from the case of $A_{xy} = 0$ are also valid for the case of $A_{xy} = 0.2$. Accordingly, the evolution properties of the degree of polarization of the partially coherent Lorentz-Gauss beam propagating in uniaxial crystals orthogonal to the x-axis are similar for the different values of A_{xy}.

4. CONCLUSIONS

Analytical expressions of the elements of the cross spectral density matrix are derived to describe the partially coherent Lorentz-Gauss beam propagating in uniaxial crystals orthogonal to the x-axis. Therefore, the intensity and degree of polarization for the partially coherent Lorentz-Gauss beam propagating in uniaxial crystals orthogonal to the x-axis can be calculated. Then the evolution properties of the partially coherent Lorentz-Gauss beam are numerically demonstrated. The influences of the uniaxial crystal and coherence length on the propagation properties of the partially coherent Lorentz-Gauss beam in uniaxial crystals orthogonal to the x-axis are examined. Here we consider that the extraordinary refractive index of the uniaxial crystal is larger than its ordinary refractive index. Upon propagation in the uniaxial crystals orthogonal to the x-axis, the spreading of the partially coherent Lorentz-Gauss beam in the direction along the x-axis is faster than that in the direction along

the y-axis, which results in the elongation of the beam spot in the direction along the x-axis. With increasing the value of n_e/n_o, the spreading of the partially coherent Lorentz-Gauss beam increases in the direction along the x-axis, but decreases in the direction along the y-axis. With increasing the coherence length, the beam spot of the partially coherent Lorentz-Gauss beam uniformly becomes less in each direction. The degree of polarization of the partially coherent Lorentz-Gauss beam displays a symmetrical distribution. The degree of polarization in the edges of the long and short axes of the beam spot reaches the maximum and second largest values, respectively. Upon propagation in the uniaxial crystals orthogonal to the x-axis, the degree of polarization in the edge of the beam spot first increases and then keeps stable without counting the expansion of the beam spot. With increasing the value of n_e/n_o, the degree of polarization in the edges of the long and short axes of the beam spot increases, and the region difference where the degree of polarization reaches the maximum value between the directions along the x- and y-axes also widens. With increasing the coherence length, the maximum degree of polarization in the edge of the beam spot decreases. This research is beneficial to the practical applications of single mode diode laser.

ACKNOWLEDGMENT

This research was supported by the National Natural Science Foundation of China under Grant No. 11574272, Zhejiang Provincial Natural Science Foundation of China under Grant No. LY16A040014, and the Scientific Research Fund of Zhejiang Provincial Education Department under Grants Nos. Y201432649 and Y201225628.

REFERENCES

1. Naqwi, A. and F. Durst, "Focus of diode laser beams: A simple mathematical model," *Appl. Opt.*, Vol. 29, 1780–1785, 1990.
2. Yang, J., T. Chen, G. Ding, and X. Yuan, "Focusing of diode laser beams: A partially coherent Lorentz model," *Proc. SPIE*, Vol. 6824, 68240A, 2008.
3. Gawhary, O. E. and S. Severini, "Lorentz beams and symmetry properties in paraxial optics," *J. Opt. A: Pure Appl. Opt.*, Vol. 8, 409–414, 2006.
4. Zhou, G., "Focal shift of focused truncated Lorentz-Gauss beam," *J. Opt. Soc. Am. A*, Vol. 25, 2594–2599, 2008.
5. Zhou, G., "Beam propagation factors of a Lorentz-Gauss beam," *Appl. Phys. B*, Vol. 96, 149–153, 2009.
6. Torre, A., "Wigner distribution function of Lorentz-Gauss beams: A note," *Appl. Phys. B*, Vol. 109, 671–681, 2012.
7. Zhou, G. and R. Chen, "Wigner distribution function of Lorentz and Lorentz-Gauss beams through a paraxial ABCD optical system," *Appl. Phys. B*, Vol. 107, 183–193, 2012.
8. Zhao, C. and Y. Cai, "Paraxial propagation of Lorentz and Lorentz-Gauss beams in uniaxial crystals orthogonal to the optical axis," *J. Mod. Opt.*, Vol. 57, 375–384, 2010.
9. Wang, X., Z. Liu, and D. Zhao, "Nonparaxial propagation of Lorentz-Gauss beams in uniaxial crystal orthogonal to the optical axis," *J. Opt. Soc. Am. A*, Vol. 31, 872–878, 2014.
10. Zhou, G., "Fractional Fourier transform of Lorentz-Gauss beams," *J. Opt. Soc. Am. A*, Vol. 26, 350–355, 2009.
11. Du, W., C. Zhao, and Y. Cai, "Propagation of Lorentz and Lorentz-Gauss beams through an apertured fractional Fourier transform optical system," *Opt. Lasers in Eng.*, Vol. 49, 25–31, 2011.
12. Zhou, G. and X. Chu, "Average intensity and spreading of a Lorentz-Gauss beam in turbulent atmosphere," *Opt. Express*, Vol. 18, 726–731, 2010.
13. Zheng, H., R. Chen, and C. H. R. Ooi, "Self-focusing dynamics of Lorentz-Gaussian beams in Kerr media," *Lasers Eng.*, Vol. 24, 345–354, 2013.
14. Keshavarz, A. and G. Honarasa, "Propagation of Lorentz-Gaussian beams in strongly nonlocal nonlinear media," *Commun. Theor. Phys.*, Vol. 61, 241–245, 2014.

15. Saraswathi, R. C., K. Prabakaran, K. B. Rajesh, and Z. Jaroszewicz, "Tight focusing properties of radially polarized Lorentz-Gaussian beam," *Optik*, Vol. 125, 5339–5342, 2014.
16. Sun, Q., A. Li, K. Zhou, Z. Liu, G. Fang, and S. Liu, "Virtual source for rotational symmetric Lorentz-Gaussian beam," *Chin. Opt. Lett.*, Vol. 10, 062601, 2012.
17. Jiang, Y., K. Huang, and X. Lu, "Radiation force of highly focused Lorentz-Gauss beams on a Rayleigh particle," *Opt. Express*, Vol. 19, 9708–9713, 2011.
18. Mandel, L. and E. Wolf, *Optical Coherence and Quantum Optics*, Cambridge University Press, Cambridge, 1995.
19. Zhou, G., "Propagation of a partially coherent Lorentz-Gauss beam through a paraxial ABCD optical system," *Opt. Express*, Vol. 18, 4637–4643, 2010.
20. Zhao, C. and Y. Cai, "Propagation of partially coherent Lorentz and Lorentz-Gauss beams through a paraxial ABCD optical system in a turbulent atmosphere," *J. Mod. Opt.*, Vol. 58, 810–818, 2011.
21. Eyyuboğlu, H. T., "Partially coherent Lorentz-Gaussian beam and its scintillations," *Appl. Phys. B*, Vol. 103, 755–762, 2011.
22. Zhou, G. and X. Chu, "M^2-factor of a partially coherent Lorentz-Gauss beam in a turbulent atmosphere," *Appl. Phys. B*, Vol. 100, 909–915, 2010.
23. Xu, Y. and G. Zhou, "Kurtosis parameter of partially coherent Lorentz-Gauss beam in turbulent atmosphere," *High Power Laser and Particle Beams*, Vol. 22, 1187–1191, 2010.
24. Zhou, G., "Generalized M^2-factors of truncated partially coherent Lorentz and Lorentz-Gauss beams," *J. Opt.*, Vol. 12, 015701, 2010.
25. Ciattoni, A., G. Cincotti, and C. Palma, "Propagation of cylindrically symmetric fields in uniaxial crystals," *J. Opt. Soc. Am. A*, Vol. 19, 792–796, 2002.
26. Lü, B. and S. Luo, "Propagation properties of three-dimensional flatted Gaussian beams in uniaxially anisotropic crystals," *Opt. Laser Technol.*, Vol. 36, 51–56, 2004.
27. Liu, D. and Z. Zhou, "Various dark hollow beams propagating in uniaxial crystals orthogonal to the optical axis," *J. Opt. A: Pure Appl. Opt.*, Vol. 10, 095005, 2008.
28. Tang, B., "Hermite-cosine-Gaussian beams propagating in uniaxial crystals orthogonal to the optical axis," *J. Opt. Soc. Am. A*, Vol. 26, 2480–2487, 2009.
29. Li, J., Y. Chen, Y. Xin, and S. Xu, "Propagation of higher-order cosh-Gaussian beams in uniaxial crystals orthogonal to the optical axis," *Eur. Phys. J. D*, Vol. 57, 419–425, 2010.
30. Zhou, G., R. Chen, and X. Chu, "Propagation of Airy beams in uniaxial crystals orthogonal to the optical axis," *Opt. Express*, Vol. 20, 2196–2205, 2012.
31. Khonina, S. N., A. A. Morozov, and S. V. Karpeev, "Effective transformation of a zero-order Bessel beam into a second-order vortex beam using a uniaxial crystal," *Laser Phys.*, Vol. 24, 056101, 2014.
32. Yumashev, K. V. and P. A. Loiko, "Depolarization in c-cut tetragonal laser crystals," *Laser Phys.*, Vol. 26, 015002, 2016.
33. Ghaffar, A. and Q. A. Naqvi, "Focusing of electromagnetic plane wave into uniaxial crystal by a three dimensional plano convex lens," *Progress In Electromagnetics Research*, Vol. 83, 25–42, 2008.
34. Hennani, S., L. Ez-Zariy, and A. Belafhal, "Transformation of finite Olver-Gaussian beams by an uniaxial crystal orthogonal to the optical axis," *Progress In Electromagnetics Research M*, Vol. 45, 153–161, 2016.
35. Wolf, E., "Unified theory of coherence and polarization of random electromagnetic beams," *Phys. Lett. A*, Vol. 312, 263–267, 2003.
36. Schmidt, P. P., "A method for the convolution of lineshapes which involve the Lorentz distribution," *J. Phys. B: At. Mol. Opt. Phys.*, Vol. 9, 2331–2339, 1976.
37. Ciattoni, A. and C. Palma, "Optical propagation in uniaxial crystals orthogonal to the optical axis: Paraxial theory and beyond," *J. Opt. Soc. Am. A*, Vol. 20, 2163–2171, 2003.
38. Born, M. and E. Wolf, *Principles of Optics*, 7th Edition, Pergamon, Oxford, 1999.
39. Gradshteyn, I. S. and I. M. Ryzhik, *Table of Integrals, Series, and Products*, Academic Press, New York, 1980.